Using Arm Swing Movements to Maintain the Walking State in a Self-Balanced Lower-Limb Exoskeleton

Omar Mounir Alaoui, Fabien Expert, Guillaume Morel, Nathanael Jarrasse

Using Arm Swing Movements to Maintain the Walking State in a Self-Balanced Lower-Limb Exoskeleton

Omar Mounir Alaoui, Fabien Expert, Guillaume Morel, Nathanaël Jarrassé

***Abstract*— This work investigates how arm swing movements measured by Inertial Motion Unit (IMU) sensors can be used to identify and maintain the walking state in a self-balanced lower-limb exoskeleton for medical use. When an exoskeleton is in a dynamical state during gait, short patterns in IMU signals (e.g. a braking movement) can be hard to extract. Therefore, by relying on a threshold-based classifier constructed upon descriptive features of actively maintained arm swing movements, it is possible to build a gait termination detection method in which the transition between the walking and standstill states occurs whenever arm movements cease, and the corresponding patterns in the IMU signals disappear. Analysis of arm IMU signals were used to identify three amplitude and coordination-based features for the classification architecture. An online implementation of this novel detection interface for maintaining the walking state was validated with 11 unimpaired participants using the Atalante exoskeleton, leading to high accuracy with less than 2% of false negatives when the arms were swinging at a high amplitude, and less than 15% when they were swinging at a medium amplitude.**

I. INTRODUCTION

In the recent years, many improvements in robotics and associated fields have made it possible to develop medical lower-limb exoskeletons with great capabilities in both assistive and rehabilitation settings. Notably, advances in mechatronics, computer technology, processing techniques, hardware components, and electronics have accompanied the emergence of exoskeletal devices from various research teams and industrials [1], [2].

However, one key challenge in the development of exoskeletons is to properly convey motion intentions through natural and intuitive control strategies, in an effort to achieve seamless integration with the patients' sensory-motor control system, and to make wearable devices be perceived as integrated parts of their bodies [3], [4].

In previous work, kinematic signals from the upper-body as recorded by three Inertial Motion Units (IMUs) were used to convey the intention of initiating gait in the self-balanced Atalante exoskeleton (Wandercraft, Paris, France) [5], by means of a supervised learning classification architecture [6]. A similar strategy can be adapted to detect the gait termination – or stopping – intention, which is defined as the transition between steady-state walking and upright standing. In unimpaired individuals, the mechanisms associated with stopping mainly involve the lower-body to produce braking forces and decelerate the whole body [7]. However, in an exoskeleton targeted at patients suffering from lower-body impairments or paralysis, gait termination cannot be initiated by an action stemming from the lower limbs.

In many crutch-based devices, walking is implemented such as steps are initiated independently. At the end of each step, the user can decide to terminate gait, and the transition to a standstill position (where both feet lie together parallel on the floor) is usually triggered from a static position through a manual input, or a sensor-based upper-body gesture – such as a backward tilt [8]–[12]. Since the Atalante exoskeleton is capable of dynamic gait without relying on a walking aid or crutches, it implements a different walking paradigm: steps are not individually handled, but gait is rather maintained until the user triggers termination through a handheld remote controller. The active swing leg finishes its current step, and the other leg is brought forward next to it, so that the robot goes back to its standstill position. While this button-based modality can be efficient, it prevents any form of natural control, and suffers from a lack of integration to the overall system.

One possibility to implement a more intuitive control interface based on upper-body kinematics would be to predefine a specific anticipatory movement, such as a backward tilt, to express the intention of stopping. A counteracting movement against the forward progression of the exoskeleton might seem intuitive, and is on par with the findings of Rum et al. [13], [14], who showed that the trunk exhibits a backward velocity towards extension during gait termination. However, the dynamics of the robot during walking make it difficult to observe small and punctual transitioning movements in kinematic data recorded by body-worn IMUs. The approach taken in the work described here was to revert the termination paradigm: rather than focusing on a short transitioning motion, it can be possible to rely on a maintained gait-related upper-body movement that would slow down or cease as an anticipation for stopping. In particular, arm swing movements can be easier to distinguish and extract from kinematic data, and be used to detect the intention of maintaining the walking state, instead of detecting its termination *per se*.

A study by Wannier et al. [15] showed that there is a strong coordination relationship between arm and leg movements during different human locomotor activities – walking, creeping, and swimming – with locked frequencies at a small integer ratio. During gait, this coordination is dependent on the walking speed [16], and has been shown to be functional: it has an overall effect on reducing energy expenditure

O. M. Alaoui, G. Morel, and N. Jarrassé are with the Institute of Intelligent Systems and Robotics, Sorbonne Université, Paris, France. O. M. Alaoui and F. Expert are with Wandercraft, Paris, France. Corresponding author email: alaoui@isir.upmc.fr. This work was supported by Wandercraft and the French state funds through CIFRE program n°2018/0378 managed by the Association Nationale Recherche Technologie.

through reductions of the angular momentum around the vertical axis, and the ground reaction moment [17]–[20]. Additionally, excessive arm swing might improve dynamic gait stability in the medio-lateral direction [21], and provide better resistance to external perturbations [22].

These findings suggest that an arm swing based approach to detect the intention of maintaining the walking state can be both relevant and natural. A threshold-based classification architecture was developed to track a set of predefined features related to the amplitude and coordination of arm movements. In such a scheme, the exoskeleton can continue walking as long as the arms exhibit coordinated high-amplitude movements in the antero-posterior plane (i.e. in the direction of walking), and gait is terminated as soon as arm movements cease, or differ from the required swinging motion. This strategy can be related to the dead-man switch approach, where a given mechanism is activated or deactivated when a specific action ceases (such as brakes in train locomotives). An experiment was conducted to evaluate the effectiveness of such a control interface in the Atalante device.

II. THE THRESHOLD-BASED CLASSIFIER

A. Descriptive features of arm swing

Descriptive features of arm swing were derived based on data collected during a preliminary experiment, in which four participants were asked to walk in the Atalante exoskeleton while displaying different levels of movement amplitudes. Further details can be found in [23].

It was hypothesized that the movements of the arms could take over the dynamic perturbations induced by the walking exoskeleton, and that discriminative features of arm swing could be extracted from the IMU signals. The features were chosen to be scalar, and derived from a 1 s sliding window with a 50% increment on the left and right arm angular velocities in the antero-posterior plane. The window size was chosen to be greater than a half-period of arm oscillations. The features were heuristically defined to capture both the amplitude of arm movements, and the anti-phase coordination between the arms.

Amplitude-based features aim at correctly detecting the presence of arm oscillations explicitly maintained by the exoskeleton user, rather than them being an effect of the robot dynamics. For a discrete signal x of length N, the Root Mean Square (RMS) is defined as:

$$RMS(x) = \sqrt{\frac{1}{N}\sum_{n=0}^{N-1} |x[n]|^2} \tag{1}$$

It is a descriptive feature that can encompass amplitude aspects of the signal. It is common to use it on IMU signals when conducting gait analyses [24].

Coordination of the arms during walk can be assessed using the normalized cross-correlation (NCC) of the angular velocity signals at lag 0 [25], [26]. Normalized cross-correlation between two real-valued discrete signals x and y of length N is defined as:

$$(x \star y)_{\text{norm}}[k] = \frac{1}{N}\sum_{n=0}^{N-1} \frac{(x[n]-\mu_x)(y[n+k]-\mu_y)}{\sigma_x \sigma_y} \tag{2}$$

where $k \in [\![0, N-1]\!]$, $y[n+k] = 0$ if $n+k > N-1$, μ_x and μ_y are the means of x and y, and σ_x and σ_y are their standard deviations. It measures the similarity between two signals x and y for different time lags or delays k. At lag 0, this is equivalent to the Pearson Correlation Coefficient. Therefore, strongly correlated signals at lag k will have normalized cross-correlation values closer to 1 (for signals in phase) or -1 (for signals in anti-phase), and poorly correlated signals will have values closer to 0.

For each window of data, it is also possible to evaluate arm coordination through the angle of the principal direction along which the data points vary. This can be achieved through Principal Component Analysis (PCA). PCA is a dimensionality reduction technique that consists in orthogonally projecting a data set onto a linear subspace that maximizes its variance [27]. PCA has been previously used to evaluate the coordination between different parts of the body during movement [28]. In the case of anti-phase movements of the arms during walking, the first principal component (PC1) of the data formed by the left and right arm angular velocities was hypothesized to be oriented in the $-45°$ direction:

$$\text{PC1} \propto \begin{bmatrix} 1 \\ -1 \end{bmatrix} \quad i.e. \quad \angle_{PC1}(x,y) = -45° \tag{3}$$

where $\angle_{PC1}(x,y)$ is the angle of the first principal component of the data formed by the x and y signals.

These features were evaluated on IMU data collected from the preliminary experiment described in [23], as seen in Fig. 1. The figure shows that all three features seem to be good candidates for a threshold-based classifier that would detect the walking intention from medium to high amplitude arm swing movements. Threshold values were empirically derived from the data.

B. The classification architecture

The threshold-based classification architecture should be able to distinguish between two possible states: the exoskeleton user is currently walking (state 1); or the exoskeleton user wishes the robot to stop (state 0). The first state should be maintained as long as the user actively swings their arms with a medium to high amplitude, and gait termination should occur when the oscillations of the arms cease, as in the dead-man switch paradigm. The classifier implements three rules based on the derived thresholds for each feature, and relies on a majority-vote scheme to decide between the two possible states – meaning that the global output of the classifier is taken as the output given by at least two out of the three rules [29].

For a window of data containing the angular velocity signals x_l and x_r, the three threshold-based rules can be summarized as follows:

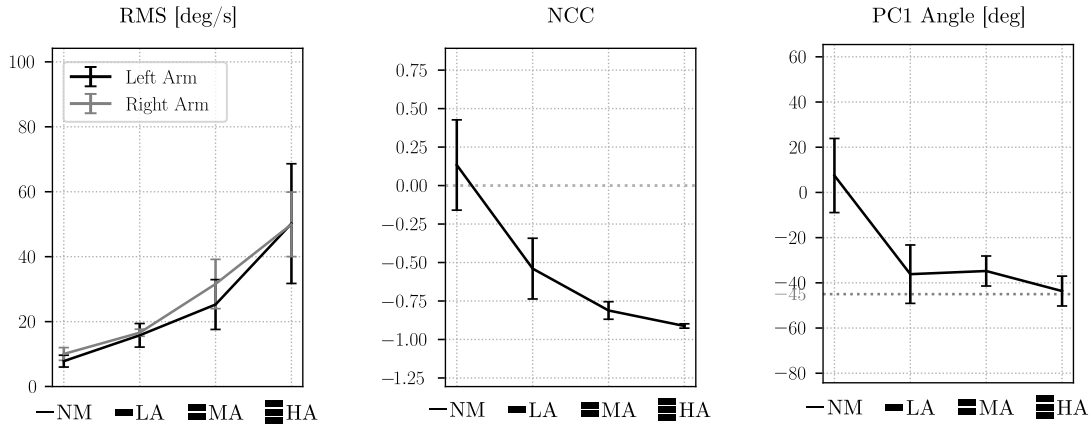

Fig. 1. Mean values of the arm swing features in four different configurations during the preliminary experiment described in [23]. The values were first averaged across all data windows for each individual configuration, and then averaged across all participants. Vertical bars represent ±1 standard deviation. The configurations are No Movement (NM, no explicitly maintained arm movements), Low, Medium, and High Amplitude (LA, MA, HA, explicitly maintained arm swing at different levels of amplitude).

$$r_{RMS}(x_l,x_r)=\begin{cases}1 \text{ if } RMS(x_l)>11°/\text{s and } RMS(x_r)>11°/\text{s}\\ 0 \text{ if } RMS(x_l)\leq 11°/\text{s or } RMS(x_r)\leq 11°/\text{s}\end{cases}$$

$$r_{NCC}(x_l,x_r)=\begin{cases}1 \text{ if } (x_l \star x_r)_{\text{norm}}[0]<-0.3\\ 0 \text{ if } (x_l \star x_r)_{\text{norm}}[0]\geq -0.3\end{cases}$$

$$r_{angle}(x_l,x_r)=\begin{cases}1 \text{ if } \angle_{PC1}(x_l,x_r)\in[-5°,-75°],\\ 0 \text{ if } \angle_{PC1}(x_l,x_r)\notin[-5°,-75°]\end{cases}$$

Therefore, the final output of the classifier is given by:

$$r(x_l,x_r)=\begin{cases}1 \text{ if } r_{RMS}(x_l,x_r)+r_{angle}(x_l,x_r)+r_{NCC}(x_l,x_r)\geq 2\\ 0 \text{ if } r_{RMS}(x_l,x_r)+r_{angle}(x_l,x_r)+r_{NCC}(x_l,x_r)<2\end{cases}$$

Additionally, in order to make the classification more robust to unwanted stops during the walk, it was required that two consecutive windows be classified as a gait termination intent before effectively stopping the robot.

III. EXPERIMENTAL VALIDATION

A. Experimental protocol and participants

An experiment was conducted to evaluate whether arm-swing movements could be used to control the maintained walking state in a lower-limb exoskeleton by relying on the threshold-based classifier. It was approved by the Ethical Committee on Research of the Paris Descartes University (IRB number 00012019-47) according to the standards of the Declaration of Helsinki. 11 unimpaired participants (7 men and 4 women) used to walking with the exoskeleton took part in the experiment. They were aged 27.5 ± 4.0 years old, with an average height of 176.6 ± 8.8 cm and an average weight of 68.0 ± 8.4 kg. They were equipped with three IMUs embedded in a jacket: one on the back, and one on each arm. The IMUs were used to record the angular velocity signals in the antero-posterior plane, with an acquisition frequency of 1 kHz. To verify the threshold-based approach, the participants were first asked to perform ten 5 m-long walks in the exoskeleton while exhibiting an exaggerated arm swing motion to express their walking intention, and terminate gait by stopping their arm movements (High Amplitude, HA). To evaluate the approach with a more natural arm swing motion, they were then instructed to complete five additional walks with normal swinging movement (Medium Amplitude, MA). The starting and ending points of the walks were marked on the ground with visible tape. For both configurations, if the exoskeleton stopped before the end of a walk, the participants were asked to resume walking to complete the 5 m distance. The failed runs were marked as unwanted stops, and the successful resumed walk was marked as a rerun. The total number of trials in each configuration corresponded to the total number of successful runs (including reruns), plus the total number of unwanted stops. The experimental procedure and the classification architecture used are illustrated in Fig. 2.

B. Data analysis

Analysis of the experimental results was primarily based on False Negatives (FNs), which corresponded to the occurrences where the exoskeleton stopped walking despite the participant still swinging their arms. Accuracy of the threshold-based architecture was therefore evaluated based on the rate of FNs among the total number of trials.

Signal data from all successful trials (excluding unwanted stops) were used to assess the amplitude of arm swing, as well as evaluate the time delays for correctly detecting gait termination after the arms have stopped swinging (which was manually labeled based on the amplitude of angular velocity signals). Analysis of the coordination and amplitude-based features values was also conducted, and their rates of wrong outputs (0 instead of 1) during walking were derived.

For comparing time delays and arm swing amplitudes between both configurations, repeated measures ANOVA tests were conducted based on the participant values averaged across trials, with the configurations as the within variable.

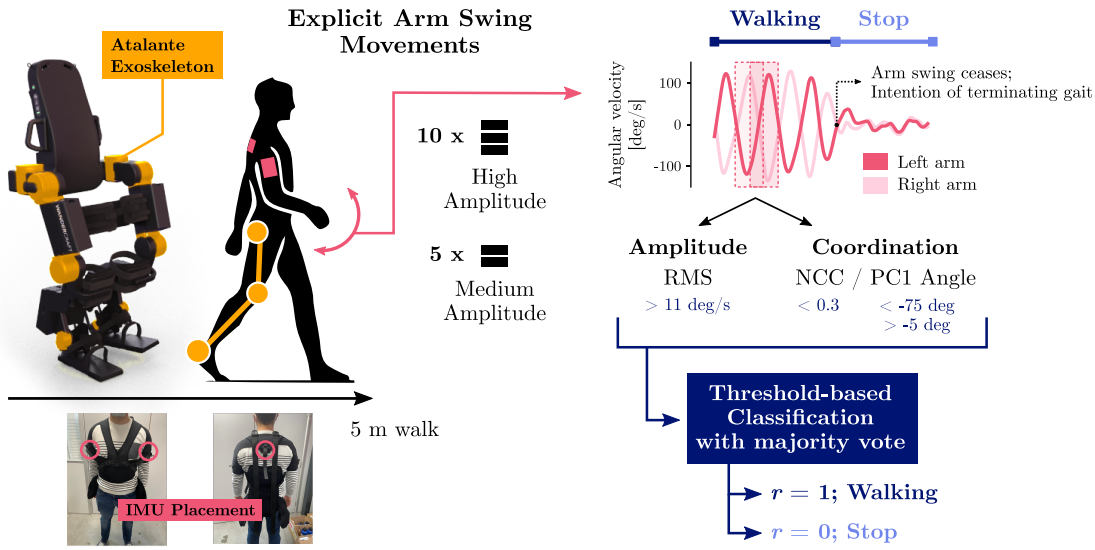

Fig. 2. Illustration of the experimental procedure and the threshold-based classification architecture.

Normality of the data was assessed using the Shapiro-Wilk test, and the repeated measures ANOVA was replaced by the non-parametric Friedman test when the normality assumption failed. Sphericity of the data was also confirmed using Mauchly's test. The same tests were used for the analysis of the individual features.

IV. RESULTS

A. Accuracy of the classification architecture

A total of 109 trials were retained for the analysis of the HA configuration. 3 trials from 2 different participants were discarded because the data revealed that the exoskeleton stopped due to a robot balance error, and not because of the classification architecture, and only 2 occurrences of FNs appeared, corresponding to a FN rate of 1.83%. In one case, the FN was due to one arm not swinging at a high enough amplitude, which affected all features. In the other, the FN was due to a loss of synchronization between both arms, which affected the coordination-based features. Example signals from the end of a successful trial can be seen on the right side of Fig. 2.

For the MA configuration, no trial was discarded. There were 8 FN occurrences: 1 in one trial from participant S2, 4 in two trials from participant S6, and 3 in two trials from participant S8. These corresponded to 5 reruns, for a total number of successful trials of 55, and a FN rate of 14.55%.

B. Analysis of gait termination detection time delays

The delay for each trial was derived as the duration between the time at which the arms have stopped swinging, and the time at which the stop event was effectively sent to the exoskeleton. Fig. 3.A shows the average delays for each participant and each configuration. The overall average was evaluated at 1.55 s for the HA configuration and 1.23 s for the MA configuration. The difference in delays was statistically significant ($p < 10^{-2}$).

C. Analysis of arm swing amplitude

Arm swing amplitude was evaluated by deriving the mean angular ranges for each participant. Fig. 3.B shows the resulting values for both configurations HA and MA. The average values across all participants were reported on the figure as dashed lines. For the left arm, they were $41.3° \pm 10.9°$ for the HA configuration and $20.6° \pm 9.2°$ for the MA configuration, and for the right arm, they were $40.2° \pm 9.6°$ for the HA configuration and $20.7° \pm 9.2°$ for the MA configuration. For both arms, the difference in mean angular ranges between both configurations was statistically significant ($p < 10^{-4}$).

D. Analysis of the performance of the classifier features

Mean values of the features were computed during walking for each trial, and then averaged across all trials for each participant. Similar derivations were applied to standard deviations, in order to evaluate the mean variations in the feature values during walking. The results for both configurations are presented in Fig. 4.

The differences in average means between both configurations were statistically significant for the RMS values of both arms ($p < 10^{-4}$) and the normalized cross-correlation feature ($p < 10^{-2}$), but not for the PC1 angle. The differences in average standard deviations were statistically significant for all features: for the RMS values of both arms, the standard deviations were higher for the HA configuration ($p < 10^{-4}$), and for the NCC and PC1 angle features, the standard deviations were higher for the MA configuration ($p < 0.05$).

Additionally, the rates of wrong outputs for each feature can be seen in table I.

V. DISCUSSION

A. Effectiveness of the threshold-based classifier architecture

These results suggest that the threshold-based classifier architecture was effective at detecting the intention to main-

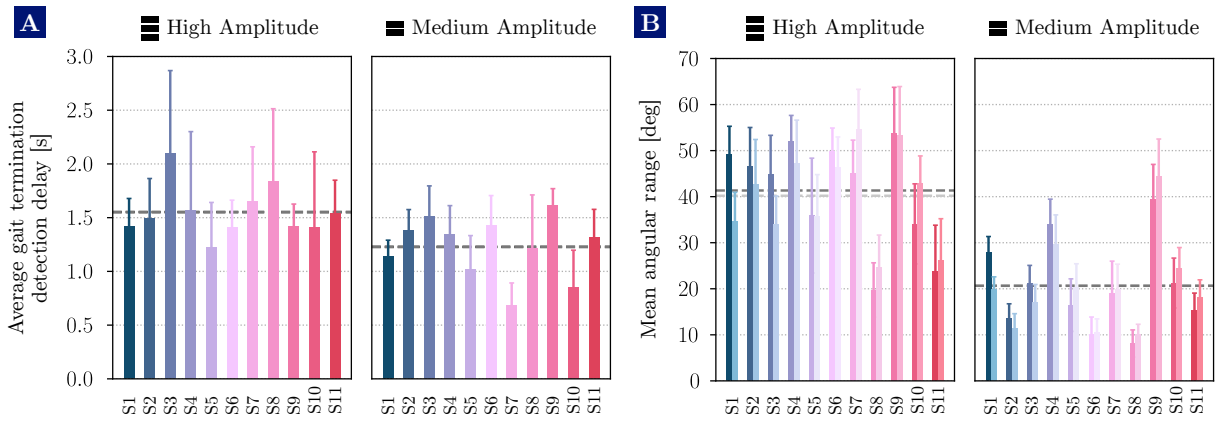

Fig. 3. A. Average gait termination intention detection delays for all participants and both configurations. B. Mean angular range of left (darker shade) and right (lighter shade) arm swing movements for all participants and both configurations. In both A and B, the dashed lines represent the averaged values across all participants (in B, darker shade for the left arm, lighter shade for the right arm).

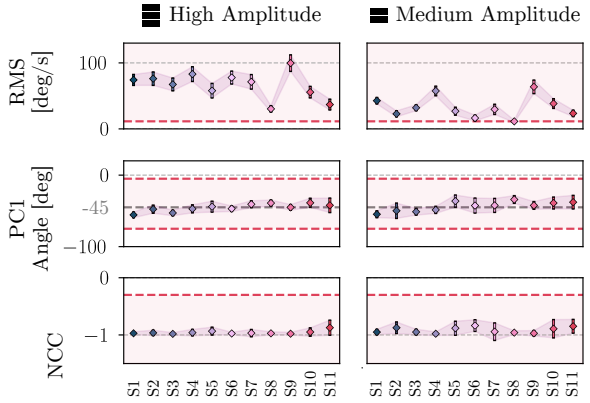

Fig. 4. Mean average values of the three features for each participant and for both configurations. For the RMS feature, only the left arm is shown. The vertical bars and shaded areas represent the average standard deviations of the corresponding features for each participant. The dashed red lines represent the threshold values for the different features.

	High Amplitude	Medium Amplitude
RMS	0.06%	4.7%
PC1 angle	0.27%	0.18%
NCC	0.18%	0.30%

TABLE I

RATES OF WRONG OUTPUTS DURING THE EXPERIMENT.

tain the walking state, with low occurrences of FNs in both amplitude configurations, and a lower rate of FNs for the HA configuration. The participants were able to lower their arm swing amplitude for the MA configuration, which was on average divided by two between both configurations: the average arm angular range was around 20°, which corresponds to the values reported in the literature for natural-speed gait [21], [30], [31]. Therefore, the proposed control interface can be effective when exhibiting arm swing movements with natural angular ranges, and could become intuitive for exoskeleton users while requiring minimal cognitive burden. However, there were no explicit instructions about arm swing frequency, and the coordination of the swinging motion with the steps. This could be enforced so that more natural movements are exhibited – for example by computing coordination features between the arms and the exoskeletal legs.

Additionally, analysis of the three different features showed that arm coordination is better when amplitude of the movements is high, with less variance in the feature values, and normalized cross-correlation coefficients closer to -1 on average. However, in both configurations, the average values for the coordination-based features were far from the thresholds used during the experiment, which could therefore be modified. On the contrary, the RMS feature showed higher variance at a high amplitude, but values closer to the threshold in the MA configuration. Exaggerated movements therefore seem to express a tighter coupling of the upper limbs, but give less control on the amplitude of arm swing.

Overall, the three features were individually effective at detecting the walking intention, with very low rates of wrong outputs: less than 1% for all features in the HA configuration, and a rate higher than 1% only for the RMS feature in the MA configuration. The higher number of FNs in the MA configuration was mostly due to low amplitudes of the arm movements, which seems to correlate with the higher rate of wrong outputs from the RMS feature (see Table I): 5 of the 6 FNs in this configuration came from participants S6 and S8, who had the lowest average RMS values, and average angular ranges of motion around 10° (see Fig. 3 and 4). More generally, wrong outputs are not evenly distributed among participants, which shows that subject-dependant parameters could be selected for an increased effectiveness of the control interface. An adaptation phase might also have played an important role in the performance of the classification, and additional training could improve its accuracy.

B. Lowering the time delay for gait termination

While the previous results confirm that the choice of features was appropriate, the time delays for the detection of gait termination intention are relatively high compared to the 0.5 s delay for planned stopping in the literature [32], with average delays higher than 1 s for both configurations.

It is important to note that this duration cannot be lower than 0.5 s, since the design of the classification algorithm requires that two successive windows output the gait termination state before effectively sending a stop signal to the exoskeleton. In many cases, when the arms stop moving, the current window can still be classified as a walking state, since it can contain data points that were recorded before the arms stopped swinging. This virtually causes a higher latency, with delays higher than 1 s (corresponding to two windows). Additionally, the inertia from the exoskeleton dynamics can cause the arms to continue swinging for a short time after the participant has ceased any explicit movements, which may introduce additional delay. This might explain why the average delay was lower for the MA configuration.

Importantly, the Atalante exoskeleton was used in a setting where one step is executed in approximately 700 ms, with a step length between 14 and 16 cm. This corresponds to terminating gait within 28 to 48 cm, which can be acceptable in settings where precise stopping is not required – such as in rehabilitation centers where exoskeletons are usually used in long walkways.

To lower the time delays before the stop event is effectively sent to the exoskeleton, possible solutions include lowering the time increment of the data windows, and fine-tuning the feature thresholds for earlier detection. This was evaluated offline using the data from the experiment, by applying different values of the window increment and threshold parameters. For different parameter combinations, the gain in time delays compared to an offline simulation with the experiment parameters was computed for each trial in both configurations. The mean and standard deviation values were derived for each participant, and then averaged across all participants. The window increment was set every 50 ms between 50 ms and 500 ms. The threshold values were set based on Fig. 4, which shows that they can be adjusted for the PC1 angle and normalized cross-correlation features. The threshold value for the RMS was not modified.

Results from this offline evaluation are shown in Fig. 5, where the rate of potential FNs for each combination was also reported. A total of three different combinations of the threshold parameters were tested. From the figure, it is clear that time delays can be successfully lowered in both configurations when the window increment is made shorter, and when the threshold values are adjusted. However, this induces higher occurrences of FNs as the window increment gets shorter, and as the thresholds allow for less variability of the feature values. In particular, combination (3) of the threshold parameters seems to highly increase the rate of FNs, even at high window increments in the MA configuration. Setting the window increment between 250 and 400 ms with combination (1) of the threshold parameters might offer a good trade-off between the gain in detection delays (around 0.5 s) and occurrences of FNs (up to 10% in the MA configuration). Additionally, it can be reasonably hypothesized that some amount of training with specific sets of parameters might reduce the number of FNs.

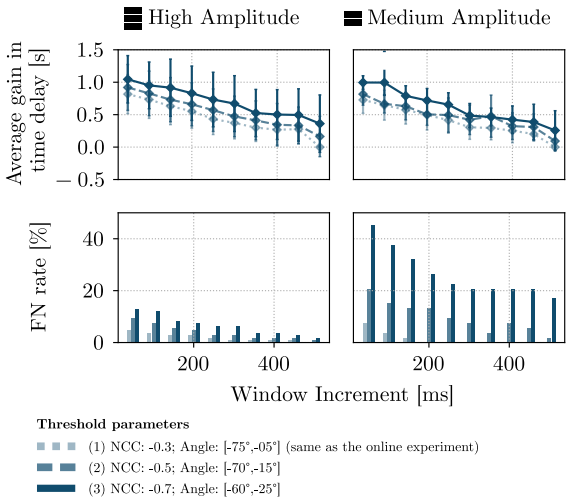

Fig. 5. *Top:* Average gain in time delays for both configurations for different combinations of the window increment and feature threshold parameters. *Bottom:* Number of FNs detected for the different combinations of parameters.

VI. CONCLUSION

Through this work, a control interface for the detection of the intention to maintain the walking state in a lower-limb exoskeleton was built. A dead-man switch approach was used to terminate gait when arm movements ceased, instead of focusing on a specific movement transition between walking and stopping. This was done by building a threshold-based classification architecture, and relying on a set of three descriptive features of arm swing amplitude and coordination.

The experimental study with the Atalante exoskeleton showed promising results for the implementation of such an interface. Participants to the experiment were able to successfully control walking and stopping in the exoskeleton with minimal unwanted stops from FNs, and arm swing amplitudes close to natural ranges. However, the control interface needs to be tested on large cohorts of patients with different pathology levels to assess whether the empirically derived thresholds for the three amplitude and coordination-based features can be generalized to all exoskeleton users. It would also be possible to implement a parametrizable user-friendly interface where individual patients could select different threshold values to adjust to their own capabilities and training levels.

Additionally, incorporating arm movements during rehabilitation of neurologically impaired individuals might be beneficial, given the growing evidence that upper and lower limbs are strongly coupled during gait-related tasks [33], [34]. Patients such as hemiplegic individuals have successfully shown their ability at actively responding to instructions and modulating their arm movements [35]. Furthermore, by involving arm rhythmic movements in rehabilitative settings, and enforcing their coordination with the exoskeleton steps, lower limb muscle activation might be enhanced [26]. This suggests that such a strategy would actively engage patients in rehabilitation settings during gait, and therefore prove to be beneficial.

REFERENCES

[1] H. Lee, P. W. Ferguson, and J. Rosen, "Lower Limb Exoskeleton Systems — Overview," in Wearable Robotics. INC, 2020, pp. 207–229.

[2] A. J. Young and D. P. Ferris, "State of the art and future directions for lower limb robotic exoskeletons," IEEE Transactions on Neural Systems and Rehabilitation Engineering, vol. 25, no. 2, pp. 171–182, 2017.

[3] M. R. Tucker, J. Olivier, A. Pagel, H. Bleuler, M. Bouri, O. Lambercy, J. R. Del Millán, R. Riener, H. Vallery, and R. Gassert, "Control strategies for active lower extremity prosthetics and orthotics: A review," Journal of NeuroEngineering and Rehabilitation, vol. 12, no. 1, 2015.

[4] W. Seymour, Remaking the Body. Routledge, feb 1998.

[5] V. Huynh, G. Burger, Q. V. Dang, R. Pelgé, G. Boeris, J. W. Grizzle, A. D. Ames, and M. Masselin, "An Efficient and Versatile Framework for Dynamic Motion Generation and Execution in Real Life Settings: Application to Atalante Evolution with a Complete Paraplegic Person at Cybathlon 2020 Exoskeleton Race," Frontiers in Robotics and AI, to be published.

[6] O. Mounir Alaoui, F. Expert, G. Morel, and N. Jarrasse, "Using Generic Upper-Body Movement Strategies in a Free Walking Setting to Detect Gait Initiation Intention in a Lower-Limb Exoskeleton," IEEE Transactions on Medical Robotics and Bionics, vol. 2, no. 2, pp. 236–247, 2020.

[7] Y. Jian, D. A. Winter, M. G. Ishac, and L. Gilchrist, "Trajectory of the body COG and COP during initiation and termination of gait," Gait & Posture, vol. 1, no. 1, pp. 9–22, 1993.

[8] K. A. Strausser and H. Kazerooni, "The development and testing of a human machine interface for a mobile medical exoskeleton," IEEE International Conference on Intelligent Robots and Systems, pp. 4911–4916, 2011.

[9] H. A. Quintero, R. J. Farris, and M. Goldfarb, "Control and Implementation of a powered lower limb orthosis to aid walking in paraplegic individuals," in 2011 IEEE International Conference on Rehabilitation Robotics, 2011, pp. 1–6.

[10] A. Esquenazi, M. Talaty, A. Packel, and M. Saulino, "The Rewalk powered exoskeleton to restore ambulatory function to individuals with thoracic-level motor-complete spinal cord injury," American Journal of Physical Medicine and Rehabilitation, vol. 91, no. 11, pp. 911–921, 2012.

[11] T. Vouga, R. Baud, J. Fasola, M. Bouri, and H. Bleuler, "TWIICE - A lightweight lower-limb exoskeleton for complete paraplegics," IEEE International Conference on Rehabilitation Robotics, pp. 1639–1645, 2017.

[12] R. Griffin, T. Cobb, T. Craig, M. Daniel, N. Van Dijk, J. Gines, K. Krämer, S. Shah, O. Siebinga, J. Smith, and P. Neuhaus, "Stepping Forward with Exoskeletons," IEEE Robotics and Automation Magazine, 2017.

[13] L. Rum, L. Laudani, A. Macaluso, and G. Vannozzi, "Upper body accelerations during planned gait termination in young and older women," Journal of Biomechanics, vol. 65, pp. 138–144, 2017.

[14] L. Rum, L. Laudani, G. Vannozzi, and A. Macaluso, "Age-related changes in upper body contribution to braking forward locomotion in women," Gait & Posture, vol. 68, no. November 2018, pp. 81–87, 2019.

[15] T. Wannier, C. Bastiaanse, G. Colombo, and V. Dietz, "Arm to leg coordination in humans during walking, creeping and swimming activities," Experimental Brain Research, 2001.

[20] B. R. Umberger, "Effects of suppressing arm swing on kinematics, kinetics, and energetics of human walking," Journal of Biomechanics, vol. 41, no. 11, pp. 2575–2580, 2008.

[16] R. E. A. Van Emmerik, R. C. Wagenaar, and E. E. H. Van Wegen, "Interlimb Coupling Patterns in Human Locomotion: Are We Bipeds or Quadrupeds?" Annals of the New York Academy of Sciences, vol. 860, no. 1, pp. 539–542, nov 1998.

[17] H. Elftman, "The function of the arms in walking," Human biology, vol. 11, no. 4, p. 529, 1939.

[18] S. M. Bruijn, O. G. Meijer, J. H. Van Dieën, I. Kingma, and C. J. C. Lamoth, "Coordination of leg swing, thorax rotations, and pelvis rotations during gait: The organisation of total body angular momentum," Gait & Posture, vol. 27, pp. 455–462, 2008.

[19] S. H. Collins, P. G. Adamczyk, and A. D. Kuo, "Dynamic arm swinging in human walking," Proceedings of the Royal Society B: Biological Sciences, vol. 276, no. 1673, pp. 3679–3688, 2009.

[21] M. Punt, S. M. Bruijn, H. Wittink, and J. H. van Dieën, "Effect of arm swing strategy on local dynamic stability of human gait," Gait & Posture, vol. 41, no. 2, pp. 504–509, 2015.

[22] S. M. Bruijn, O. G. Meijer, P. J. Beek, and J. H. Van Dieën, "The effects of arm swing on human gait stability," Journal of Experimental Biology, vol. 213, no. 23, pp. 3945–3952, 2010.

[23] O. Mounir Alaoui, "Developing a Human-Machine Control Interface for the Detection of Motion Intentions in a Self-Balanced Lower-Limb Exoskeleton," Ph.D. dissertation, Sorbonne Université, 2021.

[24] M. Sekine, T. Tamura, M. Yoshida, Y. Suda, Y. Kimura, H. Miyoshi, Y. Kijima, Y. Higashi, and T. Fujimoto, "A gait abnormality measure based on root mean square of trunk acceleration," Journal of NeuroEngineering and Rehabilitation, vol. 10, no. 1, pp. 4–8, 2013.

[25] J. L. Stephenson, A. Lamontagne, and S. J. De Serres, "The coordination of upper and lower limb movements during gait in healthy and stroke individuals," Gait & Posture, vol. 29, no. 1, 2008.

[26] D. P. Ferris, H. J. Huang, and P. C. Kao, "Moving the arms to activate the legs," Exercise and Sport Sciences Reviews, vol. 34, no. 3, pp. 113–120, 2006.

[27] C. Bishop, "Continuous Latent Variables," in Pattern Recognition and Machine Learning, 1st ed. New York: Springer-Verlag, 2006, ch. 12, pp. 559 – 603.

[28] N. St-Onge and A. G. Feldman, "Interjoint coordination in lower limbs during different movements in humans," Experimental Brain Research, vol. 148, no. 2, pp. 139–149, 2003.

[29] S. J. Preece, J. Y. Goulermas, L. P. J. Kenney, D. Howard, K. Meijer, and R. Crompton, "Activity identification using body-mounted sensors—a review of classification techniques ," Physiological Measurement, vol. 30, pp. 1–33, 2009.

[30] I. Carpinella, P. Crenna, M. Rabuffetti, and M. Ferrarin, "Coordination between upper-and lower-limb movements is different during overground and treadmill walking," European Journal of Applied Physiology, vol. 108, pp. 71—-82, 2010.

[31] A. Plate, D. Sedunko, O. Pelykh, C. Schlick, J. R. Ilmberger, and K. Bötzel, "Normative data for arm swing asymmetry: How (a)symmetrical are we?" Gait & Posture, vol. 41, no. 1, pp. 13–18, 2015.

[32] R. J. Jaeger and V. P., "Ground reaction forces during termination of human gait," Journal of Biomechanics, vol. 25, no. 10, pp. 1233–1236, 1992.

[33] P. Meyns, S. M. Bruijn, and J. Duysens, "The how and why of arm swing during human walking," Gait & Posture, vol. 38, no. 4, pp. 555–562, 2013.

[34] V. Dietz, "Quadrupedal coordination of bipedal gait: Implications for movement disorders," Journal of Neurology, vol. 258, no. 8, pp. 1406–1412, aug 2011.

[35] M. P. Ford, R. C. Wagenaar, and K. M. Newell, "Phase manipulation and walking in stroke," Journal of Neurologic Physical Therapy, vol. 31, no. 2, pp. 85–91, 2007.